Available online at www.sciencedirect.com
SCIENCE DIRECT
Journal of Solid State Chemistry 179 (2006) 2349–2355
JOURNAL OF SOLID STATE CHEMISTRY
www.elsevier.com/locate/jssc

Chemical shifts of atomic core levels and structure of $K_{1-x}Ti_{1-x}Sb_xOPO_4$, $x = 0$–0.23, solid solutions

V.V. Atuchin[a,*], O.A. Alekseeva[b], V.G. Kesler[c], L.D. Pokrovsky[a], N.I. Sorokina[a], V.I. Voronkova[d]

[a]*Laboratory of Optical Materials and Structures, Institute of Semiconductor Physics, SB RAS, Novosibirsk 630090, Russia*
[b]*X-ray Laboratory, Institute of Crystallography, RAS, Moscow 119333, Russia*
[c]*Technical Centre, Institute of Semiconductor Physics, SB RAS, Novosibirsk 630090, Russia*
[d]*Department of Physics, Moscow State University, Moscow 117234, Russia*

Received 25 January 2006; received in revised form 20 April 2006; accepted 22 April 2006
Available online 3 May 2006

Abstract

Antimony-doped $K_{1-x}Ti_{1-x}Sb_xOPO_4$, $x = 0.23$, crystals have been prepared by spontaneous nucleation from the flux in the quaternary system K_2O–TiO_2–P_2O_5–Sb_2O_5. Crystal structure observation with TEM method reveals the presence of superstructure ordering. Core level electronic parameters have been studied by X-ray photoelectron spectroscopy. Strong effect of Sb doping has been detected for inner shells of Ti^{4+} ions. Prominent decreasing of the binding energy difference Δ(O 1*s*–Ti $2p_{3/2}$) correlates with the shortening of mean oxide bond length L(Ti−O) at $x = 0.23$ that suggests increased ionicity of Ti−O bonds in $K_{1-x}Ti_{1-x}Sb_xOPO_4$ solid solutions.

PACS: 61.14.Lj; 68.47.Gh; 79.60.−i

Keywords: Sb:$KTiOPO_4$; X-ray photoelectron spectroscopy; Oxide bond length

1. Introduction

Many crystals related to $KTiOPO_4$ (KTP) family possess high electrooptical and nonlinear optical properties and are used in electrooptics and frequency conversion in visible and near-IR ranges [1,2]. A great number of new compounds with KTP-type structure have been created by isovalent substitution of metal ions into different cation positions in KTP basic framework [1]. Among others, a specific case of nonisovalent ion substitution is the formation of solid solutions $K_{1-x}Ti_{1-x}M_xOPO_4$ (M = Nb, Ta, Sb) for which the incorporation of M^{5+} cations into Ti^{4+} sites is accompanied by the process of vacancy creation at K^+ sites in KTP lattice and appearance of new K^+ positions [3–7]. The solubility limits of these solutions are comparatively high, $x = 0.11$ for Nb, 0.25 for Ta and 0.23 for Sb, and strong variation of the crystal properties is found with doping without KTP framework dropping [8]. Among the effects induced by doping of KTP with M^{5+} ions, the decrease of Curie temperature, increase of electrical conductivity, decrease of nonlinear optical susceptibility and refractive index tuning with x growing in $K_{1-x}Ti_{1-x}M_xOPO_4$ (M = Nb, Ta) crystals are reported in literature [4–10]. The information for the solutions $K_{1-x}Ti_{1-x}Sb_xOPO_4$ is very limited. Very nonlinear decreasing of Curie temperature in combination with general decay of powder second harmonic generation (SHG) signal, with some stimulation at $x = 0.05$, have been detected on antimony content increasing [8,9,11]. Structure analysis produced for a set of $K_{1-x}Ti_{1-x}Sb_xOPO_4$ ($x = 0$−0.17), crystals displays the splitting of K^+ positions and noticeable transformations of TiO_6 octahedra induced by Sb incorporation into KTP lattice [7]. In the present work, the effects of high-level antimony doping on crystal structure ordering and electronic properties are

*Corresponding author. Fax: +7 383 3332771.
E-mail address: atuchin@thermo.isp.nsc.ru (V.V. Atuchin).

0022-4596/$ - see front matter © 2006 Elsevier Inc. All rights reserved.
doi:10.1016/j.jssc.2006.04.025

studied by using TEM and X-ray photoelectron spectroscopy (XPS) methods. To see the limiting case of the solution, promising for most prominent variation of core level characteristics, the crystals $K_{1-x}Ti_{1-x}Sb_xOPO_4$, $x = 0.23$, have been evaluated.

2. Experimental methods

The single crystals of $K_{1-x}Ti_{1-x}Sb_xOPO_4$, $x = 0.23$, have been grown with spontaneous nucleation from the flux in the quaternary system K_2O–TiO_2–P_2O_5–Sb_2O_5 [11]. High purity $NH_4H_2PO_4$, TiO_2, Sb_2O_3 and K_2CO_3 reagents were taken for charge preparation. The crystals grown were of light yellow color and 1–3 mm in diameter. Optically clear crystals have been selected for the following observation. The chemical composition was determined using a CAMEBAX SX-50 energy dispersive X-ray (EDS) microanalyzer with primary electron excitation at an accelerating voltage of 15 kV and at a beam current of 30 nA. Crystal composition measured by this method was $K_{0.66}Ti_{0.62}Sb_{0.23}PO_{4.64}$.

Selected area electron diffraction was carried out on a BS 513A microscope operating by 100 kV. Thin crystal fragments were prepared by gentle dry grinding of Sb:KTP crystals and supported on a tungsten grid covered with holey carbon film.

Core level electronic parameters were defined with XPS method for Sb:KTP powder pressed into In substrate. XPS spectra were obtained with a MAC-2 (RIBER) analyzer using nonmonochromatic Mg $K\alpha$ radiation (1253.6 eV). The diameter of X-ray beam was ~5 mm. The energy resolution of the instrument was chosen to be 0.5 eV, so as to have sufficiently small broadening of natural core level lines together with reasonable signal–noise ratio. Under the conditions the observed full-width at half-maximum (FWHM) of the Cu $2p_{3/2}$ line was 1.4 eV. The binding energy scale was calibrated in reference to Cu $3p_{3/2}$ (75.1 eV) and Cu $2p_{3/2}$ (932.7 eV) lines, giving the accuracy of 0.1 eV in any peak energy position determination. Photoelectron energy drift due to charging effects was taken into account in reference to the position of C 1*s* (284.6 eV) line generated by adventitious carbon on the surface of powder as-inserted into the vacuum chamber.

3. XPS results

To increase the robustness of the analysis, the measurements of photoemission spectra have been produced two times for two independently prepared Sb:KTP powder samples I and II in parallel with the single-crystal sample of pure (001) KTP observed previously [12]. In Fig. 1 the survey spectra are shown for these three samples. The spectrum recorded for KTP shows only spectral features typical for clean surface of this crystal [12]. The extra lines detected for Sb:KTP at ~37 eV and ~16 eV are related to Sb 4*d* and In 4*d* core levels. Both the spectra of the Sb:KTP samples display complex multicomponent structures in any

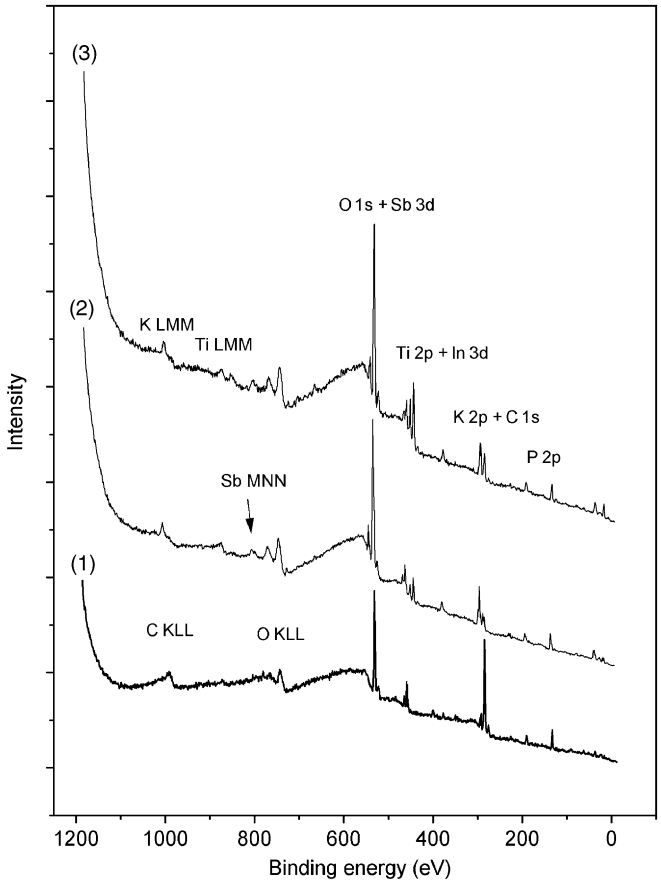

Fig. 1. Survey photoelectron spectra for pure KTP (1) and Sb:KTP II (2) and I (3).

spectral window in which a particular line related to a constituent element should be expected. The only exception is the single component In 3*d* doublet due to signal from indium substrate. In Fig. 2 this situation is illustrated for K 2*p*–C 1*s* window. So, it was supposed that we have a differential charging effect of Sb:KTP powder particles and measured spectrum is a superposition of several spectra shifted in energy. As it appears, the powder samples contain several fractions different in particle dimensions with better contact to In substrate and, respectively, weaker charging effect under X-ray illumination for smaller fraction. From the evaluation of C 1*s* signal (Fig. 2) the existence of two components for this line with energy difference 3.2 eV is evident. It should be pointed that similar two-component structure of C 1*s* band has been revealed for Sb:KTP II sample with slightly smaller energy separation 2.0 eV between the components. Thus, the spectrum recorded for Sb:KTP I can be considered as a superposition of two spectrums *A* and *B* shifted in energy by 3.2 eV. The binding energy (BE) 284.6 eV, that is typical value for C 1*s* signal of adventitious carbon in our XPS chamber, was taken for lower binding energy component of C 1*s* doublet measured for Sb:KTP I. This binding energy calibration yields the value 443.7 eV for the binding energy of In $3d_{5/2}$ component that well relates to that of

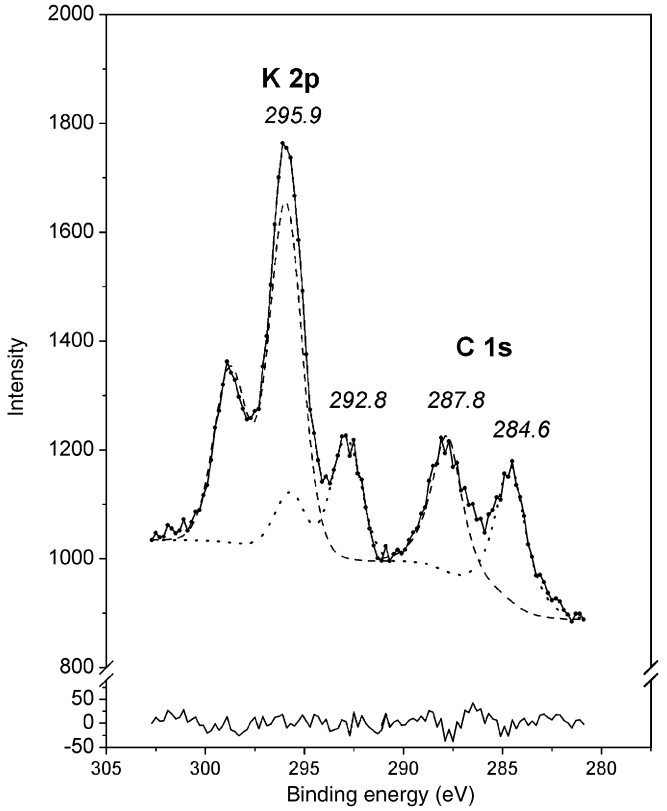

Fig. 2. Detailed spectra of K 2*p*–C 1*s* window for Sb:KTP I. Spectrums A and B related to different fractions are shown by dashed and doted lines.

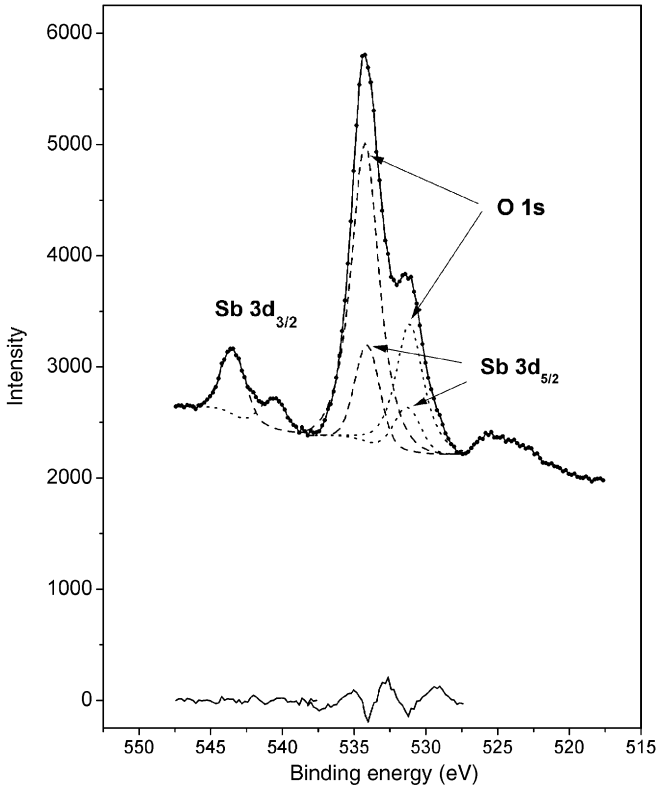

Fig. 3. Detailed spectra of Sb 3*d*–O 1*s* window for Sb:KTP I. Spectrums *A* and *B* are shown by dashed and doted lines.

indium metal [13]. It is well known, however, that indium metal surface is not stable when it contacts air and oxidation up to In_2O_3 is proceeding with time. So, let us test for the presence of In_2O_3 in our samples. The binding energy difference (O 1*s*–In $3d_{5/2}$) = 85.7 eV is a characteristic value of In_2O_3 [13]. Then, if the oxidation of In substrate happens during the Sb:KTP sample preparation, the spectrum of O 1*s* window should display a component at 529.4 eV related to In_2O_3. The inspection of O 1*s* band presented in Fig. 3 reveals the absence of noticeable additive photoemission at 529.4 eV, that confirms the presence of only In metal in the sample Sb:KTP I.

As a next step, the photoelectron spectra recorded were deconvolved under the supposition that every complex band related to a particular constituent element is generated by the contributions of two individual components *A* and *B* separated by 3.2 and 2.0 eV, respectively, for Sb:KTP I and Sb:KTP II samples. During the calculations, the FWHM for each spectral feature, besides Sb 3*d* lines, were taken equal to those recorded in the spectrum of pure KTP. The intensity ratio of components *A* and *B* was free. The results of such deconvolution for C 1*s* and O 1*s* core levels and K 2*p* and Sb 3*d* doublets are shown in Figs. 2 and 3. The binding energy of In $3d_{5/2}$ core level obtained for Sb:KTP II sample was 443.8 eV that confirms the validity of our deconvolution model. All spectral features defined for separated spectrums of Sb:KTP were successfully attributed to the constituent elements. The scatter of binding energy values found for a particular core level in these four separated spectrums was 0–0.2 eV that is not above error range possible in our XPS measurements. The exceptions are O 1*s* and Sb $3d_{5/2}$ core levels for which the scattering range is slightly larger, ~0.4 eV. As it seems, this is a result of more complicated nature of the band recorded in the binding energy range 529–537 eV that is a superposition of two O 1*s* and two Sb $3d_{5/2}$ components. In Table 1 the FWHM and averaged binding energies and Auger parameters for the representative core levels in Sb:KTP crystal are reported. The relative element contents calculated on the basis of representative element peak areas and relative element sensitivities taken from Ref. [14] are presented in Table 2. The chemical composition of powder Sb:KTP found with XPS is in good relation with the results of EDS analysis.

Table 1
Binding energies (*E*) and Auger parameters (α) for the constituent elements of $K_{0.66}Ti_{0.62}Sb_{0.23}PO_{4.64}$ crystal

Parameter, eV	O 1*s*	Ti $2p_{3/2}$	K 2*p*	P 2*p*	Sb $3d_{5/2}$	Sb $3d_{3/2}$
E	531.2	459.4	292.8	133.2	531.2	540.5
FWHM	2.24	1.8	1.7	2.02	2.07	2.07
α	—	—	543.3	1984.7	—	—

Table 2
Averaged relative element concentrations defined by XPS in comparison with nominal composition $K_{0.66}Ti_{0.62}Sb_{0.23}PO_{4.64}$

Element	O	Ti	K	P	Sb
Core level	O 1*s*	Ti $2p_{3/2}$	K 2*p*	P 2*p*	Sb $3d_{5/2}$
C	0.67	0.07	0.10	0.14	0.023
Nominal	0.64	0.10	0.10	0.13	0.03

Table 3
Binding energy (BE) of Sb $3d_{3/2}$ core level in antimony oxides

BE, eV	Oxides			References
	Sb_2O_3	Sb_2O_5	Sb_2O_4	
	539.0	539.8	—	[15]
	538.9	539.9	539.8 + 539.3	[16]
	539.4	540.0	539.6	[17]
	539.13	—	—	[18]

The values presented in original papers are rescaled in reference to BE (C 1*s*) = 284.6 eV.

There is a possibility to consider Sb valence state in $K_{0.77}Ti_{0.77}Sb_{0.23}PO_5$ by comparison of the binding energy of Sb $3d_{3/2}$ core level with earlier reported data for simple antimony oxides Sb_2O_3, Sb_2O_5 and Sb_2O_4. It is well known that the states Sb^{3+} and Sb^{5+} are possible for antimony in oxide compounds. Then the Sb_2O_3 and Sb_2O_5 oxides can be good representatives for individual Sb^{3+} and Sb^{5+} states and Sb_2O_4 possesses the simultaneous presence of both Sb^{3+} and Sb^{5+} ions with a one-to-one ratio. The values of binding energy of Sb $3d_{3/2}$ core level measured for the oxides are collected in Table 3. It is very appropriate that the observations of the sets of different oxides were produced in the same experiment, this opens the possibility to minimize the difference between the spectrometers used. The difference between the binding energies of Sb $3d_{3/2}$ lines found for Sb_2O_3 and Sb_2O_5 vary within the range 0.6–1.0 eV and, respectively, the states Sb^{3+} and Sb^{5+} can be well separated with XPS method. Quality of the measurements is confirmed by the following details. The value of BE of Sb $3d_{3/2}$ level in Sb_2O_4 for the integrated case ($Sb^{3+} + Sb^{5+}$) should be between those in Sb_2O_3 and Sb_2O_5 with individual antimony valence states. This relation is confirmed experimentally in Ref. [17]. The spectral components related to Sb^{3+} and Sb^{5+} states in Sb_2O_4 were separated in Ref. [16] and those correlate well with the values defined for Sb_2O_3 and Sb_2O_5. Furthermore, mean value of BEs of Sb $3d_{3/2}$ line in Sb_2O_3 measured in Ref. [15–17] accords well with the BE value specified in most recent experiment [18]. Thus, we can reasonably use these data reported in literature for antimony oxides for the comparison. In our experiment the value of BE of Sb $3d_{3/2}$ line is 540.5 eV that confirms the presence of only valence state Sb^{5+} in $K_{0.77}Ti_{0.77}Sb_{0.23}PO_5$.

4. Electron microscopy

Selected area electron diffraction (SAED) patterns for $K_{0.77}Ti_{0.77}Sb_{0.23}PO_5$ shown in Figs. 4 and 5 can be indexed in orthorhombic unit cell with $a_0 = 1277.6(2)$ pm, $b_0 = 641.02(9)$ pm, $c_0 = 1055.027(6)$ pm found for Sb:KTP solid solution $K_{0.83}Ti_{0.83}Sb_{0.07}OPO_4$ with the chemical composition closest to our sample [7]. For ED pattern shown in Fig. 4(a) the experimental value of *d*-spacing found for vertical direction is 1066 pm and this direction is identified as [001] with superstructure relation $c = 4c_0$. Indexation of this SAED pattern is presented in the inset in Fig. 4(a). There is a traditional problem for KTP-type materials with identification of crystallographic direction orthogonal to [001]. Because of the relation $a_0 \cong 2b_0$ specific for unit cell of all crystals related to KTP family and possibility of superstructure ordering with even indices [19,20], it is not possible to distinguish uniquely the directions [100] and [010] in SAED patterns. Indeed, the experimental *d*-spacing in the side direction is 640 pm and, if we consider this direction as [010], then superstructure ordering is defined by the relation $b = 2b_0$ and Variant I is workable. Another way is to interpret the side direction as [100] in SAED pattern shown in Fig. 4. In this case the relation $a = a_0$ is valid and Variant II should be considered. Fig. 5 displays the SAED pattern for $(\bar{2}11)$ and related indexation is presented in the inset.

These and other SAED patterns recorded for our sample $K_{0.77}Ti_{0.77}Sb_{0.23}OPO_4$ display the presence of only reflexes related to KTP-type lattice. There was no any traces detected of foreign crystaline phases or prominent amor-

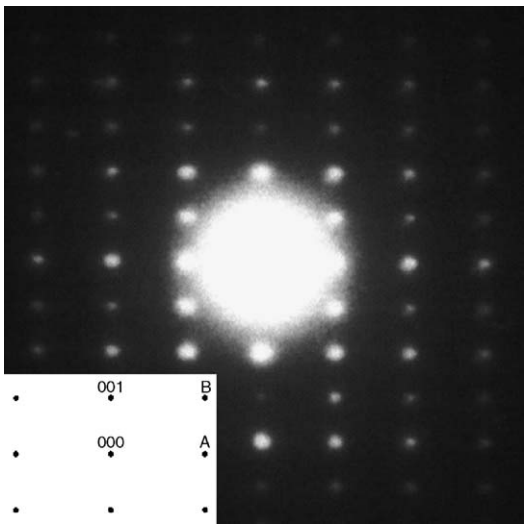

(a)

Reflex	A	B
Variant I	010	011
Variant II	200	201

(b)

Fig. 4. SAED pattern of $K_{0.77}Ti_{0.77}Sb_{0.23}PO_5$ (a) with indexation (b) for the plane (100) or (010).

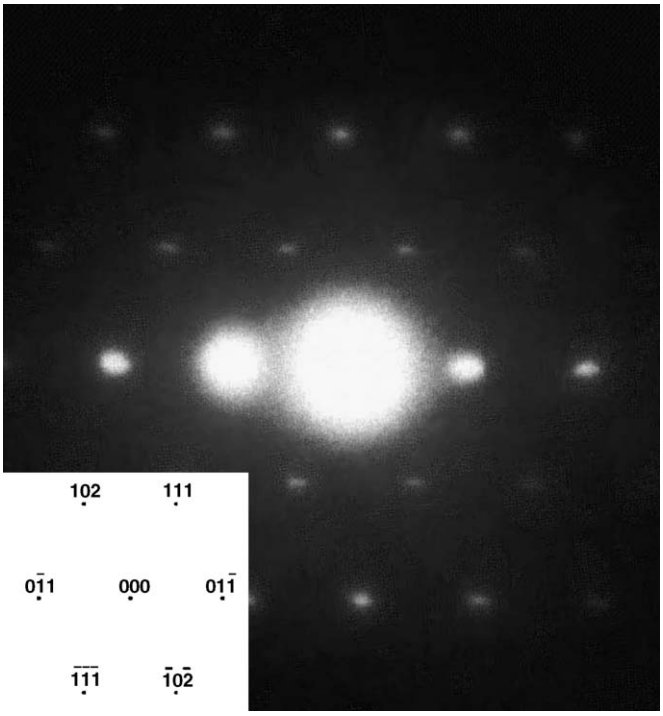

Fig. 5. SAED pattern of $K_{0.77}Ti_{0.77}Sb_{0.23}PO_5$ and indexing for the ($\bar{2}11$).

phous inclusions for as high Sb content as $x = 0.23$, upper solubility limit of $K_{1-x}Ti_{1-x}Sb_xOPO_4$ solutions.

5. Discussion

Now the core level photoemission spectral features are determined for three members of KTP crystal family, $KTiOPO_4$ [12], $TlTiOPO_4$ [19] and $K_{0.77}Ti_{0.77}Sb_{0.23}OPO_4$, and the correlation between chemical bond lengths and core level binding energies can be considered. The KTP-type framework is constructed by linked TiO_6 octahedra and PO_4 tetrahedra with covalent oxide bonds and KO_n polyhedra with ionic bonds. When metal interacts with oxygen, great redistribution of electronic density occurs as a shift of valence electrons from metal atom to oxygen resulting in noticeable variations of electronic structure of inner shells of cation and anion. The effective displacement of valence electron density away from atomic nucleus results in reduction of electrical screening of inner shells with increasing of inner electrons binding energies. This effect can be detected as a variation of core level binding energies in XPS spectra with as great magnitude as few electronvolts if we compare the electronic parameters of pure metals and fluorides for which the ionicity of chemical bonds is the highest [14]. Within the oxides, however, the difference is not so pronounced and more sensitive parameters are necessary to quantify the effect. As it was demonstrated in several studies performed for different oxides the energy difference Δ(O–M) between the representative metal core level and O 1s level is a more robust parameter for chemical bonding characterization [19,21–23]. Additionally, the variation of the energy difference is more prominent because of opposite sign of the chemical shifts of binding energies of metal and oxygen core levels when valence electrons transfer occurs from metal to oxygen ions. The shift of electron density on M–O bond formation can be characterized by mean value of the chemical bond length L(M–O) [24].

Previously it has been shown by comparison of $KTiOPO_4$ and $TlTiOPO_4$ that very small variations of L(P–O) and L(Ti–O) happening when K is substituted by Tl in KTP framework result in the persistence of Δ(O 1s–Ti 2$p_{3/2}$) and Δ(O 1s–P 2p) values [19]. An example of $K_{1-x}Ti_{1-x}Sb_xOPO_4$ solid solutions is a principally different case, because the introduction of Sb^{5+} ions into Ti sites induces great decreasing of L(Ti–O) value [7]. At the same time only slight variation of L(P–O) from 153.85 to 153.7 pm has been detected in the solutions within the doping range $x = 0-0.17$. The dependencies of L(M–O) (M = K, P, Ti) on Sb content in $K_{1-x}Ti_{1-x}Sb_xOPO_4$, $x = 0-0.17$, are presented in Fig. 6. Here, when L(K–O) values were calculated for every intermediate x value by using single crystal structure data from Ref. [7], partial occupancies of the individual potassium sites were accounted for. Experimental points can be well interpolated by linear function for P and second-order polynomials for K and Ti that permits accurate determination of L(M–O) values at $x = 0.23$ by extrapolation. The resulted values of L(M–O) (M = K, P, Ti) at $x = 0.23$ are collected in Table 4.

Table 5 contains the electronic characteristics, available now for three members of KTP crystal family. The variations of averaged ionicity of covalent oxide bond can be characterized by the value of energy difference Δ(O–M). Indeed, there is no significant influence of Sb doping of KTP on the mean bond length L(P–O) and, respectively, no any variation of binding energy difference

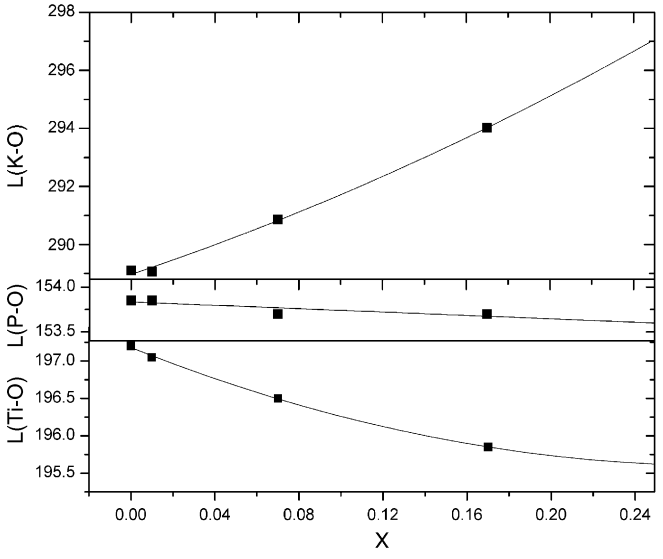

Fig. 6. Dependences of L(M–O) (M = K, P and Ti) mean bond lengths on chemical composition in solid solutions $K_{1-x}Ti_{1-x}Sb_xOPO_4$ [7].

Table 4
Mean bond lengths $L(M–O)$ in representative compounds from KTP family

$L(M–O)$, pm	$KTiOPO_4$ [25]	$TlTiOPO_4$		$K_{0.77}Ti_{0.77}Sb_{0.23}PO_5$ [this study]
		[26]	[27]	
Ti–O	197.2	197.0	197.7	195.66
P–O	153.9	153.4	153.7	153.6
K–O	289.1	—	—	296.3

Table 5
Binding energy differences for KTP type crystals

Δ(O 1s–M), eV	$KTiOPO_4$ [12]	$TlTiOPO_4$ [19]	$K_{0.77}Ti_{0.77}Sb_{0.23}PO_5$ [this study]
O 1s–Ti 2$p_{3/2}$	72.5	72.3	71.8
O 1s–P 2p	398.1	397.9	398.0
O 1s–K 2p	238.5	—	238.4

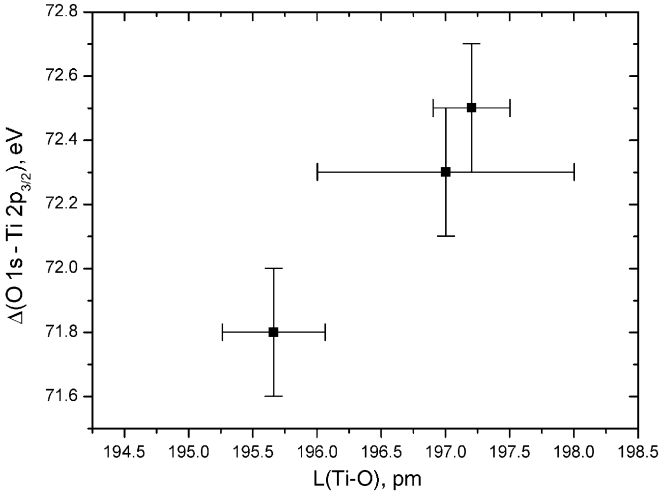

Fig. 7. Dependence of Δ(O 1s–Ti 2$p_{3/2}$) on L(Ti–O) for KTP family crystals.

Δ(O 1s–P 2p) is observed in XPS experiment. From the other hand, strong decreasing of L(Ti–O) on KTP doping by Sb results in pronounced reduction of Δ(O 1s–Ti 2$p_{3/2}$), so the bonds between Ti and O become more ionic on Sb incorporation. Earlier similar tendency in Δ(O 1s–Nb 3$d_{5/2}$) variation has been detected for Nb–O bonds [23]. The values of Δ(O 1s–Ti 2$p_{3/2}$) for KTP family crystals are displayed in Fig. 7 as a function of L(Ti–O). This dependence seems be universal and may be used for prediction of electronic characteristics of KTP-type compounds on the basis of crystal structure parameters. For example, the value of L(Ti–O) = 196.67 pm has been found for $K_{0.89}Ti_{0.89}Nb_{0.11}OPO_4$ [4,5] and respectively the value of Δ(O 1s–Ti 2$p_{3/2}$) parameter for this crystal should be an intermediate between those of $TlTiOPO_4$ and $K_{0.77}Ti_{0.77}Sb_{0.23}OPO_4$. Large values of L(Ti–O), however, have been found for $(Rb_{0.89}Cs_{0.11})TiOPO_4$, 197.8 pm [28], $RbTiOPO_4$, 197.9 pm [25], $RbTiOAsO_4$, 198.1 pm [25], $CsTiOAsO_4$, 198.9 pm [25,29], and $Na_{0.5}Rb_{0.5}Sn_{0.5}Ti_{0.5}OPO_4$, 204 pm for mixed Ti/Sn positions [30]. It is expected that the level of Δ(O 1s–Ti 2$p_{3/2}$) for the compounds should be above that of $KTiOPO_4$.

As to P−O bonds in $K_{0.89}Ti_{0.89}Nb_{0.11}OPO_4$, the value L(P–O) = 153.9 pm [4,5] lie in narrow range typical for KTP framework and, respectively, the value Δ(O 1s–P 2p) ~398 eV should be valid for Nb:KTP. For other crystals discussed above the values of L(P–O) are in the range 153.7–154.4 pm [25,28–30] and the relation Δ(O 1s–P 2p) ~398 eV seems be proper for the compounds.

It is very interesting to consider the effect of Sb doping on the oxide bonding of K for which a complete transfer of valence electron to oxygens should be supposed. The refinements of the crystal structure of $K_{1-x}Ti_{1-x}Sb_xOPO_4$ crystals show, besides the formation of two new sites for K ions, a continuous and great increasing of L(K–O) on x growing [7], as illustrated by Fig. 6. Contrary to that, the value of Δ(O 1s—K 2p) remains practically the same (see Table 5), in spite of the drastic crystal lattice transformation. So, the persistance of Δ(O 1s–K 2p) value on L(K–O) variation is a good example illustrating the principle that electronic parameters of alkali metal oxide bond seems be less sensitive to variation of the bond length.

6. Conclusions

Observation of the electronic properties of $K_{1-x}Ti_{1-x}Sb_xOPO_4$ solid solutions at high doping level $x = 0.23$ shows that a substitution of Sb for the pair (K + Ti) in KTP framework generates strong variation of inner shell parameters of Ti^{4+} ions with keeping the core level parameters of K^+ ions. The shortening of mean oxide bond length L(Ti−O) with doping is accompanied by decreasing of the binding energy difference Δ(O 1s–Ti 2$p_{3/2}$) that is an indication of increased ionicity of Ti−O bonding in Sb:KTP. From the other hand no variation of electronic properties has been observed for K^+ ions forming very ionic oxide bonds despite strong elongation of L(K−O) with Sb incorporation. So, only chemical elements with covalent oxide bonds are sensitive to redistribution of electron density on doping. Reasonably it should be supposed that noticeable shifts of electronic parameters will be observed when KTP doping with different elements results in strong variation of metal–oxygen bond lengths, excepting alkali and alkali–earth metals for which oxide bonds are very ionic.

References

[1] L.K. Cheng, J.D. Bierlein, Ferroelectrics 142 (1993) 209–228.
[2] M.E. Hagerman, K.R. Poeppelmeier, Chem. Mater. 7 (1995) 602–621.
[3] P.A. Thomas, B.E. Watts, Solid State Commun. 73 (1990) 97–100.

[4] T.Yu. Losevskaya, O.A. Alekseeva, V.K. Yanovskii, V.I. Voronkova, N.I. Sorokina, V.I. Simonov, S.Yu. Stefanovich, S.A. Ivanov, S. Eriksson, S.A. Zverkov, Crystallogr. Rep. 45 (2000) 739–743.
[5] O.A. Alekseeva, N.I. Sorokina, I.A. Verin, T.Yu. Losevskaya, V.I. Voronkova, V.K. Yanovskii, V.I. Simonov, Crystallogr. Rep. 48 (2003) 205–211.
[6] K.B. Hutton, R.C. Ward, C.F. Rae, M.H. Dunn, P.A. Thomas, C. Eaton, Proc. SPIE 3928 (2000) 77–85.
[7] O.A. Alekseeva, O.D. Krotova, N.I. Sorokina, I.A. Verin, T.Yu. Losevskaya, V.I. Voronkova, V.K. Yanovskii, V.I. Simonov, Crystallogr. Rep. 50 (2005) 554–565.
[8] V.I. Voronkova, V.K. Yanovskii, T.Yu. Losevskaya, S.Yu. Stefanovich, S.A. Zver'kov, O.A. Alekseeva, N.I. Sorokina, Crystallogr. Rep. 49 (2004) 123–129.
[9] V.I. Voronkova, V.K. Yanovskii, T.Yu. Losevskaya, S.Yu. Stefanovich, J. Appl. Phys. 94 (2003) 1954–1958.
[10] G. Zhang, D. Zhang, H. Shen, W. Liu, C. Huang, L. Huang, Y. Wei, Opt. Commun. 241 (2004) 503–506.
[11] T.Yu. Losevskaya, V.K. Yanovskii, V.I. Voronkova, S.Yu. Stefanovich, Inorg. Mater. 38 (2002) 1164–1167.
[12] V.V. Atuchin, V.G. Kesler, N.Yu. Maklakova, L.D. Pokrovsky, V.N. Semenenko, Surf. Interface Anal. 34 (2002) 320–323.
[13] D.T. Clark, T. Fok, G.G. Roberts, R.W. Sykes, Thin Solid Films 70 (1980) 261–283.
[14] D. Briggs, M.P. Seach, Practical Surface Analysis by Auger and X-ray Photoelectron Spectroscopy, Wiley, Chichester, New York, Brisbane, Toronto, Singapore, 1983.
[15] W.E. Morgan, W.J. Stec, J.R. Van Wazer, Inorg. Chem. 12 (1973) 953–955.
[16] T. Birchall, J.A. Connor, I.H. Hillier, J. Chem. Soc. Dalton Trans. (1975) 2003–2006.
[17] R. Delobel, H. Baussart, J.-M. Leroy, J. Chem. Soc. Faraday Trans. I 79 (1983) 879–891.
[18] T. Honma, R. Sato, Y. Benino, T. Komatsu, V. Dimitrov, J. Non-Cryst. Solids 272 (2000) 1–13.
[19] V.V. Atuchin, L.D. Pokrovsky, V.G. Kesler, N.Yu. Maklakova, V.I. Voronkova, V.K. Yanovskii, Surf. Rev. Lett. 11 (2004) 191–198.
[20] V.V. Atuchin, N.Yu. Maklakova, L.D. Pokrovsky, V.N. Semenenko, Opt. Mater. 23 (2003) 363–367.
[21] Y. Fukuda, M. Nagoshi, T. Suzuki, Y. Namba, Y. Syono, M. Tachiki, Phys. Rev. B 39 (1989) 11494–11497.
[22] L. O'Mahony, T. Curtin, D. Zemlyanov, M. Mihov, K. Hodnett, J. Cat. 227 (2004) 270–281.
[23] V.V. Atuchin, I.E. Kalabin, V.G. Kesler, N.V. Pervukhina, J. Elect. Spect. Rel. Phenom. 142 (2005) 129–134.
[24] V.I. Nefedov, N.P. Sergushin, Ja.V. Salyn, J. Elect. Spect. Rel. Phenom. 8 (1976) 81–84.
[25] P.A. Thomas, S.C. Mayo, B.E. Watts, Acta Crystallogr. B 48 (1992) 401–407.
[26] M. Jannin, C. Kolinsky, G. Godefroy, B. Jannot, N.I. Sorokina, D.Y. Lee, V.I. Simonov, V.I. Voronkova, V.K. Yanovskii, Eur. J. Solid State Inorg. Chem. 33 (1996) 607–621.
[27] W.T.A. Harrison, T.E. Gier, G.D. Stucky, A.J. Schultz, Mater. Res. Bull. 30 (1995) 1341–1349.
[28] Liu Wen, V.I. Voronkova, V.K. Yanovskii, N.I. Sorokina, I.A. Verin, V.I. Simonov, Crystallogr. Rep. 45 (2000) 380–385.
[29] J. Protas, G. Marnier, B. Boulanger, B. Menaert, Acta Crystallogr. C 45 (1989) 1123–1125.
[30] S.J. Crennell, A.K. Cheetham, J.A. Kaduk, R.H. Jarman, J. Mater. Chem. 2 (1992) 785–792.